Mineralogical Magazine, December 2016, Vol. 80(7), pp. 1149–1160

Penberthycroftite, $[Al_6(AsO_4)_3(OH)_9(H_2O)_5]\cdot 8H_2O$, a second new hydrated aluminium arsenate mineral from the Penberthy Croft mine, St. Hilary, Cornwall, UK

I. E. Grey[1,*], J. Betterton[2], A. R. Kampf[3], C. M. Macrae[1], F. L. Shanks[4] and J. R. Price[5]

[1] CSIRO Mineral Resources, Private bag 10, Clayton South, Victoria 3169, Australia
[2] Haslemere Educational Museum, 78 High Street, Haslemere, Surrey GU27 2LA, UK
[3] Mineral Sciences Dept., Natural History Museum of Los Angeles County, 900 Exposition Boulevard, Los Angeles, CA 90007, USA
[4] School of Chemistry, Monash University, Clayton, Victoria 3800, Australia
[5] Australian Synchrotron, 800 Blackburn Road, Clayton, Victoria 3168, Australia

[*Received 2 September 2015; Accepted 8 December 2015; Associate Editor: Giancarlo Della Ventura*]

ABSTRACT

Penberthycroftite, ideally $[Al_6(AsO_4)_3(OH)_9(H_2O)_5]\cdot 8H_2O$, is a new secondary aluminium arsenate mineral from the Penberthy Croft mine, St. Hilary, Cornwall, England, UK. It occurs as tufts of white, ultrathin (sub-micrometre) rectangular laths, with lateral dimensions generally < 20 μm. The laths are flattened on {010} and elongated on [100]. The mineral is associated with arsenopyrite, bettertonite, bulachite, cassiterite, chalcopyrite, chamosite, goethite, liskeardite, pharmacoalumite–pharmacosiderite and quartz. Penberthycroftite is translucent with a white streak and a vitreous to pearly lustre. The calculated density is 2.18 g/cm^3. Optically, only the lower and upper refractive indices could be measured, 1.520(1) and 1.532(1) respectively. No pleochroism was observed. Electron microprobe analyses (average of 14) with H_2O obtained from thermogravimetric analysis and analyses normalized to 100% gave Al_2O_3 = 31.3, Fe_2O_3 = 0.35, As_2O_5 = 34.1, SO_3 = 2.15 and H_2O = 32.1. The empirical formula, based on nine metal atoms and 26 framework anions is $[Al_{5.96}Fe_{0.04}(As_{0.97}Al_{0.03}O_4)_3(SO_4)_{0.26}(OH)_{8.30}(H_2O)_{5.44}](H_2O)_{7.8}$, corresponding to the ideal formula $[Al_6(AsO_4)_3(OH)_9(H_2O)_5]\cdot 8H_2O$. Penberthycroftite is monoclinic, space group $P2_1/c$ with unit-cell dimensions (100 K): a = 7.753(2) Å, b = 24.679(5) Å, c = 15.679(3) Å and β = 94.19(3)°. The strongest lines in the powder X-ray diffraction pattern are [d_{obs} in Å(I) (*hkl*)] 13.264(46)(011); 12.402(16)(020); 9.732(100)(021); 7.420(28)(110); 5.670(8)(130); 5.423(6)($\bar{1}$31). The structure of penberthycroftite was solved using synchrotron single-crystal diffraction data and refined to wR_{obs} = 0.059 for 1639 observed ($I > 3\sigma(I)$) reflections. Penberthycroftite has a heteropolyhedral layer structure, with the layers parallel to {010}. The layers are strongly undulating and their stacking produces large channels along [100] that are filled with water molecules. The layers are identical to those in bettertonite, but they are displaced relative to one another along [001] and [010] such that the interlayer volume is decreased markedly (by ~10%) relative to that in bettertonite, with a corresponding reduction in the interlayer water content from 11 H_2O per formula unit (pfu) in bettertonite to 8 H_2O pfu in penberthycroftite.

Introduction

We have recently described (Grey *et al.*, 2014*a*, 2015*b*) a new secondary hydrated aluminium arsenate mineral, bettertonite, $[Al_6(AsO_4)_3(OH)_9(H_2O)_5]\cdot 11H_2O$, from the Penberthy Croft mine located in the parish of St, Hilary, Cornwall (50.1414°N, 5.4269°W). Other hydrated aluminium arsenate minerals reported at Penberthy Croft mine are mansfieldite and liskeardite (Betterton, 2000; Grey *et al.*, 2013). In ongoing studies of minerals associated with bettertonite we

* E-mail: Ian.Grey@csiro.au
DOI: 10.1180/minmag.2016.080.069

encountered another hydrated aluminium arsenate, which was initially thought to be bulachite, $Al_2(AsO_4)(OH)_3.3H_2O$ (Walenta, 1983), as it had in common with this mineral the same [Al]/[As] atomic ratio and a similar powder X-ray diffraction pattern. Further studies, however, including a single-crystal structure determination, confirmed that the link with bulachite was fortuitous and that the new mineral was a distinct species with a structure related to that of bettertonite. We report here the characterization of the new mineral, penberthycroftite.

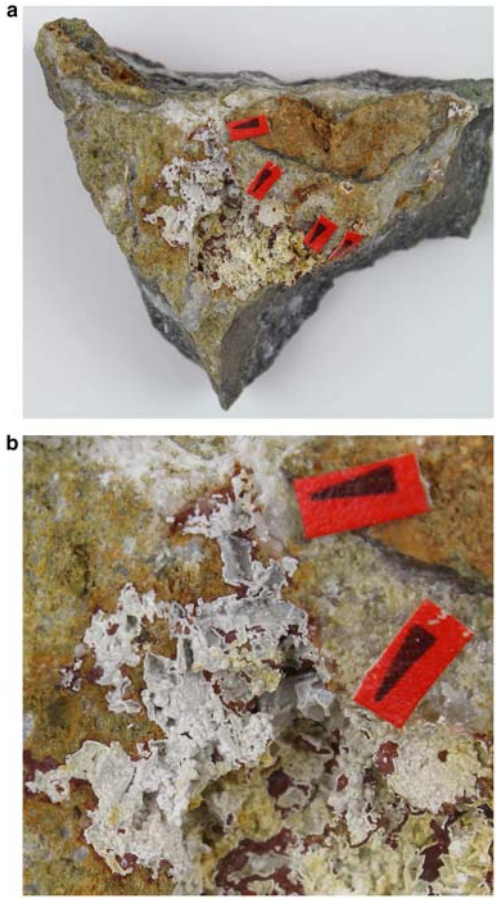

FIG. 1. (*a*). Optical image of penberthycroftite (white) on quartz (white to grey, translucent), chamosite (weathered, greenish yellow) and goethite (brown). Cream to yellow crusts at bottom right of the cavity contain mixtures of penberthycroftite with other aluminium arsenate minerals. Field of view is ~6 cm. The arrows show where samples were excavated for study. (*b*) A higher magnification image of white penberthycroftite crusts, field of view ~1.7 cm. Specimen Number PC240. John Betterton Collection. Image Robert Neller.

The mineral and name have been approved by the IMA Commission on New Minerals, Nomenclature and Classification (2015-025, Grey *et al.*, 2015*a*). The mineral is named for the location where the mineral was found, Penberthy Croft mine. The full name penberthycroftite has been used, rather than the abbreviated penberthyite, to avoid confusion with the numerous Penberthy families who once worked in the mining industry throughout Cornwall. The mine was worked for copper and tin in the 18th and 19th centuries and was designated a Site of Special Scientific Interest in 1993 for its mineralization. The mine is well known for its diverse range of secondary arsenate minerals, particularly Cu-Pb-Fe arsenates. These include bayldonite, $PbCu_3(AsO_4)_2(OH)_2{\cdot}H_2O$, which was the only type mineral from the mine prior to the discovery of bettertonite (Betterton, 2000). Co-type specimens are housed in the mineralogical collections of Museum Victoria, Melbourne, Victoria, Australia, registration number M53452 and the Natural History Museum, London, registration number BM. 2015,3.

Occurrence

The geology and mineralization at Penberthy Croft have been described by Betterton (2000) and Bevins *et al.* (2010). The arsenate mineral assemblage at Penberthy Croft is interpreted as having formed from prolonged oxidation of various sulfides in the upper parts of lodes and veins within the mine and on dump material (Betterton, 2000). Characteristic residual gossans present due to extensive supergene alteration and acidic leaching, resulted in rich Fe-Mn oxides, hydroxides and quartz assemblages that hosted the various arsenate suites, and also display extreme local variations in morphology and colour (Taylor, 2011).

Specimens containing penberthycroftite were collected by one of the authors (JB) during the early 2000s in two separate areas, ~700 m apart, of the mine dumps. A small specimen measuring 6.2 cm × 4.9 cm in size consists of a single open cavity in massive vein quartz measuring ~2 cm × 2.2 cm in size, shown in Fig. 1*a*. The quartz matrix of this specimen contains small areas of fresh massive chamosite, but much has been weathered extensively to an earthy goethite and is never in direct contact with penberthycroftite. Minor scattered patches of massive to granular cassiterite occur, along with massive chalcopyrite, spherical scorodite and minute crystals of pharmacosiderite. The mineral occurs as cavity fillings and as thin crusts

https://doi.org/10.1180/minmag.2016.080.069 Published online by Cambridge University Press

of tufted and sometimes interconnected crystalline aggregates (Fig. 1*b*), also in parts developing into protruding structures and clusters. It is a notable feature that the penberthycroftite has grown only on an ultra-thin layer of a reddish iron oxide (goethite), which in turn is on the quartz. Elsewhere on this specimen, penberthycroftite occurs as an intimate and extremely complex mixture of bettertonite, liskeardite, bulachite and pharmacosiderite–pharmacoalumite solid solutions in various proportions.

The mineral also occurs in groups in small cavities completely infilled with bright white, dense lath-like crystal aggregates within a matrix of quartz, chamosite and arsenopyrite. The cavity infillings also possess ultra-thin boundaries forming boxwork-like networks across the cavities. The thin boundaries consist mostly of light green chamosite and white to clear quartz, and are just visible under the optical microscope at x70 magnification in most examples. In incomplete cavities, vugs are lined with microscopic transparent to translucent tufts of penberthycroftite. The mineral also occurs as thin crusts on vein quartz. Penberthycroftite is a much rarer mineral species at Penberthy Croft than the higher hydrate, bettertonite.

Paragenesis

A general review of the paragenesis of arsenic minerals present in various mineralogical deposits including those within supergene and mine dump environments is given by Bowell *et al.* (2014). The primary minerals most probably involved in aluminium arsenate mineral paragenesis at Penberthy Croft mine and their abundance are: arsenopyrite (abundant) for As, and chamosite (frequent), muscovite (minor) and orthoclase (minor) for Al. That arsenopyrite is the source for As appears to be confirmed by occurrences of penberthycroftite, intimately mixed with other Al-arsenate species (bettertonite, liskeardite, pharmacoalumite/pharmacosiderite and bulachite), in aggregates resembling a boxwork cellular network with regular- to irregular-shaped cells after arsenopyrite. Here, euhedral and anhedral areas of arsenopyrite have been leached completely out by acidic waters and replaced by the various Al-arsenates, faithfully preserving their original crystal outlines in some sections of the specimens. They form a type of isoalteromorph where the volume of the secondary minerals is equal to that of the primary mineral and where its external outline and size are preserved. All species here tend to be poorly crystallized and may represent incomplete reactions that occurred fairly rapidly on these specimens in the mine dump environment that has preserved remnants of each of the Al-arsenates. Together they form a complex paragenesis that is newly described for this locality.

Bettertonite, $[Al_6(AsO_4)_3(OH)_9(H_2O)_5]\cdot 11H_2O$ and penberthycroftite, $[Al_6(AsO_4)_3(OH)_9(H_2O)_5]\cdot 8H_2O$, differ only in their degree of hydration and it is possible that one derives from the other by hydration/dehydration reactions. In separate *in situ* synchrotron

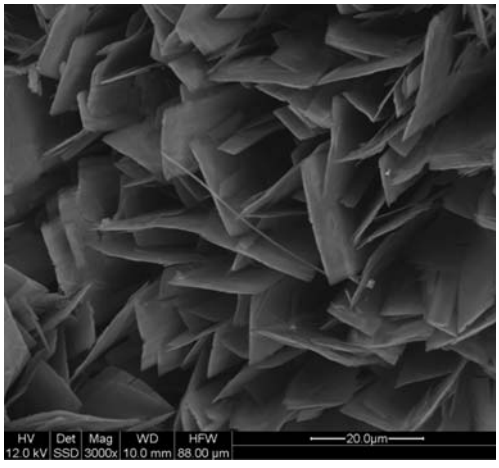

FIG. 2. Back-scattered electron (BSE) image of penberthycroftite laths.

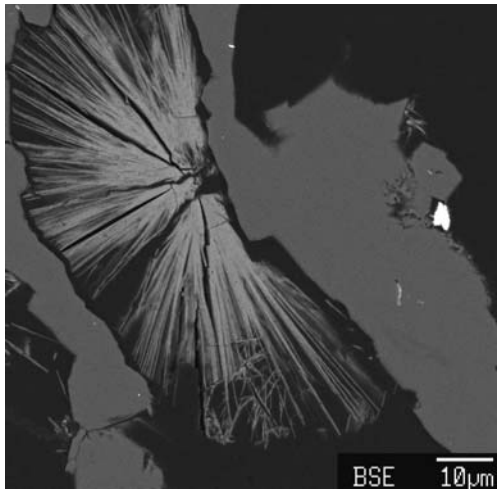

FIG. 3. BSE image of sprays of penberthycroftite laths, viewed edge-on in the polished section used for electron microprobe analyses. The darker mineral is quartz.

https://doi.org/10.1180/minmag.2016.080.069 Published online by Cambridge University Press

heating studies we have observed that bettertonite is transformed to penberthycroftite by heating in the temperature range 65 to 85°C. The transformation is reversible in character.

Appearance, physical and optical properties

Penberthycroftite occurs as bright white coloured tufts and sprays of ultrathin (sub-micrometre) rectangular or bladelike laths, with lateral dimensions generally <20 μm long, shown in Fig. 2. The laths are flattened on {010} and are elongated along [100]. Figure 3 shows sprays of laths viewed edge-on, which radiate out from a relatively dense base. On some specimens, penberthycroftite is present together with several other Al-arsenates species, namely bettertonite, liskeardite, bulachite and pharmacosiderite–pharmacoalumite forming an intimate and extremely complex mixture in various proportions. These crusts are off-white to pale cream in colour with slight variations in tint. Crusts consist of tufted laths and sometimes-interconnected aggregates with a dull and nearly waxy lustre.

Penberthycroftite is translucent with a white streak and a vitreous to pearly lustre. It shows perfect basal cleavage on {010}. The crystals are flexible, with irregular fracture. The mineral is non-fluorescent under both short- and long-wavelength ultraviolet radiation. The calculated density is 2.18 g/cm^3 using the empirical formula.

Penberthycroftite proved to be very difficult to work on optically. The laths are so thin and narrow that it is difficult to properly observe Becke lines and the sprays of laths remain clumped together even when attempts are made to separate them. The laths have parallel extinction and are length slow. The lower index of refraction is 1.520(1) and the upper index is 1.532(1), based more upon relief than Becke line observations. There was no pleochroism and dispersion could not be observed. A Gladstone-Dale calculation (Mandarino, 1981) gave a compatibility index of –0.033 (excellent), for the empirical formula using the density derived from the single-crystal X-ray data and the average of the upper and lower indices of refraction.

Other properties

Thermogravimetric analysis

Thermogravimetric analysis was performed on a 1.8 mg sample using a Netzsch STA 449 F1 Jupiter Simultaneous TGA/DSC thermal analyser. The analysis was performed in dry air, with a ramp rate of 10°C/min, between 30 and 600°C. Evolved gas analysis was made using a coupled Thermostar Pfeiffer mass spectrometer. Two endotherms corresponding to water evolution were recorded at 94 and 180°C, and an endotherm due to SO_3 evolution occurred at 481°C. No AsO_x gaseous species were detected. The total mass loss was corrected for admixed quartz (the amount of quartz was quantified using Rietveld phase analysis) and for evolved SO_3 to obtain the water content, as 32.1 wt.% H_2O.

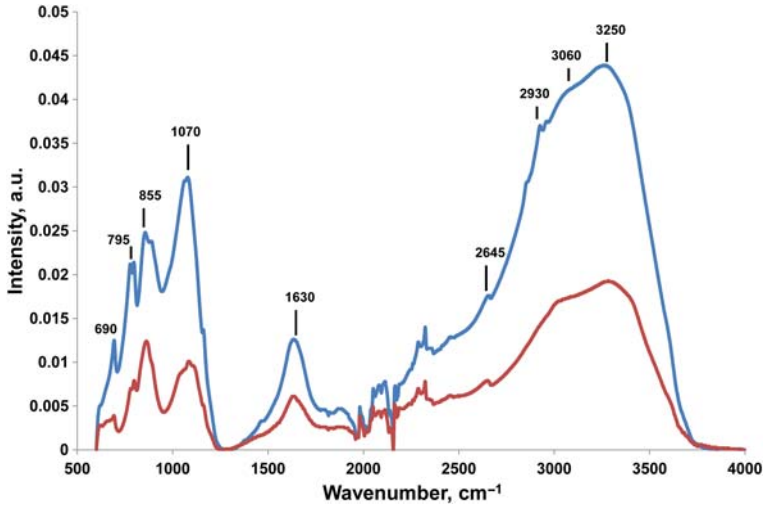

FIG. 4. Infrared spectra for penberthycroftite (lower curve) and bettertonite (upper curve).

https://doi.org/10.1180/minmag.2016.080.069 Published online by Cambridge University Press

Infrared spectroscopy

Diamond attenuated total reflection infrared spectra in the range 600 to 4000 cm^{-1} were made on powder samples using a Bruker IFS 55 Fourier transform IR instrument, fitted with an MCT detector, and 100 co-added scans were used with a spectral resolution of 4 cm^{-1}. The IR spectra for penberthycroftite and bettertonite are compared in Fig. 4 (the vertical scale depends on pressing efficiency). The two spectra are very similar. A broad band extending from ~3600 to 2500 cm^{-1}, with a number of weak sharp peaks superimposed on the hump, corresponds to O–H stretching vibrations from strongly H-bonded water and hydroxyl, while an H–O–H bending vibration at 1630 cm^{-1} confirms significant water concentrations in both minerals. A peak at 1070 cm^{-1} can be assigned to the triply degenerate ν3 asymmetric stretching vibration for $(SO_4)^{2-}$. For the free sulfate molecule, ν3 is at 1105 cm^{-1} (Nakamoto, 1970). Majzlan *et al*. (2011) report that ν3 occurs as a broad band centred at 1062–1071 cm^{-1} in hydrated iron sulfate minerals. The ν4 bending vibration for $(SO_4)^{2-}$ is at 690 cm^{-1}. Both the ν3 and ν4 peaks for $(SO_4)^{2-}$ are much broader and shows splitting in penberthycroftite relative to bettertonite. In the region for As–O stretching vibrations, 700–900 cm^{-1} (Vansant *et al*., 1973), two doublets are observed, with main peaks at 855 and 795 cm^{-1} and shoulders at 884 and 775 cm^{-1}. Similar doublets were reported by Frost *et al*. (2015) for the arsenate mineral tangdanite. They assigned the higher wavenumber doublet to ν1 symmetric stretching and the lower wavenumber doublet to ν3 antisymmetric stretching vibrations. Pairs of doublets at 853/838 and 774/750 cm^{-1} have also been reported for As–O stretching vibrations in ianbruceite, $Zn_2(AsO_4)(OH)\cdot 3H_2O$ (Cooper *et al*. 2012).

Chemical analysis

Crystals of penberthycroftite were analysed using wavelength-dispersive spectrometry on a JEOL JXA 8500F Hyperprobe operated at an accelerating voltage of 12 kV and a beam current of 2 nA. The beam was defocused to 1 μm. As is typical of highly hydrated phases with weakly held H_2O, penberthycroftite partially dehydrates under vacuum in the electron microprobe. This H_2O loss results in higher concentrations of the remaining constituents than are to be expected for the fully hydrated phase. The water content was analysed directly by thermogravimetric analysis and the electron microprobe analyses were then normalized to give a total of 100%. Analytical results from analysis of 14 crystals (14 analyses) are given in Table 1.

The empirical formula based on nine framework metals (Al + Fe + As) and 26 framework anions, with OH^-/H_2O adjusted to give charge balance is: $[Al_{5.96}Fe_{0.04}(As_{0.97}Al_{0.03}O_4)_3(SO_4)_{0.26}(OH)_{8.30}(H_2O)_{5.44}](H_2O)_{7.8}$. The simplified formula is $[Al_6(AsO_4)_3(OH)_9(H_2O)_5]\cdot 8H_2O$.

Crystallography

Powder X-ray diffraction

Finely ground penberthycroftite was packed in a 0.3 mm diameter quartz glass capillary for powder X-ray diffraction data collections, which were conducted on the powder diffraction beamline at the Australian Synchrotron. High energy 18 kV X-rays were used to reduce fluorescence due to As. The wavelength was 0.68824 Å, calibrated to NIST standard LaB_6 660b. The capillary was positioned in the diffractometer rotation centre and spun at ~1 Hz. The X-ray beam was aligned to coincide with the diffractometer centre. The data were collected using

TABLE 1. Electron microprobe compositional data for penberthycroftite.

Constituent	wt.%	Range	SD	Norm. wt.%	Probe Standard
Al_2O_3	37.6	35.9–41.1	1.5	31.3	$AlPO_4$
Fe_2O_3	0.42	0–0.82	0.28	0.35	scorodite
As_2O_5	41.0	38.3–43.9	1.6	34.1	scorodite
SO_3	2.58	1.83–3.32	0.49	2.15	pyrite
H_2O*				32.1	
Total				100.0	

*From thermogravimetric analysis.

https://doi.org/10.1180/minmag.2016.080.069 Published online by Cambridge University Press

TABLE 2. Powder X-ray diffraction data for penberthycroftite.

I_{rel}	d_{meas} (Å)	d_{calc} (Å)	h	k	l	I_{rel}	d_{meas} (Å)	d_{calc} (Å)	h	k	l
46	**13.264**	**13.267**	**0**	**1**	**1**	2.5	3.459	3.458	$\bar{2}$	2	2
16	**12.402**	**12.394**	**0**	**2**	**0**	6	3.402	3.404	2	3	1
100	**9.732**	**9.732**	**0**	**2**	**1**	5	3.310	3.310	2	4	0
1.5	7.777	7.778	1	0	0	2	3.059	3.058	0	8	1
28	**7.420**	**7.423**	**1**	**1**	**0**	2	3.030	3.030	$\bar{1}$	7	2
3	7.316	7.318	0	3	1	2	3.019	3.019	2	1	3
1	6.637	6.640	0	2	2	1	2.991	2.991	2	5	1
1	6.209	6.211	$\bar{1}$	2	1	2	2.971	2.971	1	7	2
2.5	5.734	5.734	$\bar{1}$	0	2	2	2.885	2.884	$\bar{2}$	4	3
4	5.695	5.701	0	3	2	3	2.839	2.839	1	8	1
8	**5.670**	**5.670**	**1**	**3**	**0**	1	2.800	2.801	$\bar{1}$	7	3
1	5.588	5.587	$\bar{1}$	1	2	2	2.734	2.734	0	9	1
6	**5.423**	**5.423**	**$\bar{1}$**	**3**	**1**	4	2.710	2.710	$\bar{1}$	4	5
3	5.354	5.353	1	0	2	4	2.687	2.688	0	8	3
5	4.498	4.499	1	3	2	1	2.652	2.652	0	7	4
2	4.010	4.009	0	6	1	2	2.624	2.624	$\bar{2}$	7	1
2	3.896	3.892	0	1	4	1	2.558	2.559	3	2	0
1	3.763	3.762	$\bar{1}$	5	2	2	2.549	2.550	$\bar{1}$	7	4
1	3.683	3.679	$\bar{2}$	2	1	1	2.541	2.542	$\bar{2}$	7	2
4	3.663	3.663	1	6	0	3	2.522	2.523	$\bar{3}$	1	2
6	**3.598**	**3.598**	**$\bar{2}$**	**0**	**2**	2	2.435	2.435	0	4	6
6	**3.562**	**3.562**	**$\bar{2}$**	**1**	**2**	3	2.367	2.366	3	4	1
2	3.546	3.544	1	6	1	2	2.270	2.270	$\bar{2}$	0	6
2.5	3.495	3.495	$\bar{2}$	3	1	1	2.239	2.239	2	9	1
4	3.478	3.479	$\bar{1}$	2	4						

The strongest lines are given in bold.

a Mythen position sensitive detector covering 80° in 2θ with a resolution of 0.004° in 2θ. Pairs of data sets were collected at two detector positions 0.5° apart in order to cover the gaps between the detector modules. Acquisition time at each position was 300 s. The data pairs were merged into single files using in-house data processing software, *PDViPcR*, available at the beamline.

The powder pattern was indexed using the Ito method (Visser, 1969) with a monoclinic cell having similar parameters as for bettertonite but with an 8% shrinkage in the *b* parameter. Refinement of 49 2θ values using *CELLREF* (Laugier and Bochu, 2000) gave the following cell parameters: $a = 7.789(2)$, $b = 24.777(4)$, $c = 15.737(3)$ Å, $\beta = 93.960(1)°$ and $V = 3029.7(1.0)$ Å^3. The indexed powder lines are reported in Table 2.

Single-crystal studies

A rectangular lath, measuring ~0.03 mm × 0.01 mm × 0.001 mm was used for a data collection at 100 K on the microfocus beamline MX2 at the Australian Synchrotron, λ = 0.7100 Å. The extreme thinness and curvature of the crystal resulted in very weak diffraction data (average I/σ(I) = 3.2) and a high mosaicity.

The structure was solved using *SHELXT* (Sheldrick, 2008) within the *WinGX* program suite (Farrugia, 2012) and refined using *JANA2006* (Petříček and Dušek, 2006). All the atoms in the heteropolyhedral layers and four interlayer water molecules were found by *SHELXT*. Partially occupied water molecule sites and a partially occupied SO_4 molecule were located in difference Fourier maps. The partially occupied sites were constrained to have the same isotropic displacement parameter, and the S and its coordinating anions were constrained to have the same site occupation factor, which was refined. The large number of atoms in the unit cell (large number of refinable parameters), coupled with the relatively low resolution of the data, restricted the refinement of displacement parameters to isotropic values. The

https://doi.org/10.1180/minmag.2016.080.069 Published online by Cambridge University Press

TABLE 3. Crystal data and structure refinement for penberthycroftite.

Formula	$[Al_6(AsO_4)_3(OH)_9(H_2O)_5]\cdot 8H_2O$
Temperature	100 K
Wavelength	0.7100 Å
Crystal system	Monoclinic
Space group	$P\ 2_1/c$
Unit-cell dimensions	$a = 7.753(2)$ Å $b = 24.679(5)$ Å $c = 15.679(3)$ Å $\beta = 94.19(3)°$.
Volume	2991.9(12) $Å^3$
Z	4
Density (calculated)	2.18 g/cm^3
Absorption coefficient	3.57 mm^{-1}
Absorption correction	*SADABS*, T_{min}, T_{max} 0.48, 0.75
Crystal size	0.03 mm × 0.01 mm × 0.001 mm
Theta range	1.5 to 30.1°
Index ranges	$-10 \le h \le 10$, $-34 \le k \le 34$, $-22 \le l \le 22$
Reflections collected	53,235
Independent reflections	2934 [$R(int) = 0.19$]
Refinement method	Full-matrix least-squares on F
Data / restraints / parameters	2934 / 10 / 190
Reflections with $I > 3\sigma(I)$	1639
Final R indices [$I > 3\sigma(I)$]	$R_{obs} = 0.068$, $wR_{obs} = 0.059$
R indices (all data)	$R_{obs} = 0.145$, $wR_{obs} = 0.066$
Largest diff. peak and hole	0.68 and –0.67 $e.Å^{-3}$

refinement converged at $wR_{obs} = 0.059$ for 1639 unique reflections with $I > 3\sigma(I)$ and 190 refined parameters. Further details of the refinement are given in Table 3. The refined coordinates, isotropic displacement parameters and site occupancies are given in Table 4. Included in Table 4 are bond-valence sums (BVS) calculated in *JANA2006*. Polyhedral bond lengths are reported in Table 5.

Discussion

Penberthycroftite has a layer structure, with the crankshaft-like stepped layers parallel to (010) as shown in Fig. 5. The layers comprise hexagonal rings of edge-shared Al-centred octahedra that are interconnected by corner-sharing with AsO_4 tetrahedra as illustrated in Fig. 6. The layers are identical to those in bettertonite, shown in Fig. 7, but they are displaced relative to one another along [001] and [010] such that the interlayer volume is decreased by ~10% relative to that in bettertonite, with a corresponding reduction in the interlayer water content from 11 H_2O per formula unit (pfu) in bettertonite to 8 H_2O pfu in penberthycroftite. In addition to water molecules, the interlayer region contains a partially occupied SO_4 anion that coordinates to a terminal anion of one of the Al-centred octahedra as shown in Fig. 5. Bettertonite has almost the same SO_3 content as penberthycroftite but in the refinement of bettertonite the sulfate molecules could not be located. This may be because in the more widely spaced layer structure of bettertonite the sulfate molecules are disordered over a number of different sites.

The empirical formula for penberthycroftite, normalized to nine metal atoms, has an excess of Al + Fe and an equivalent deficiency of As of 0.09 atoms. We have previously observed a deficit of As and excess of Al in bariopharmacoalumite, and have confirmed from the structure refinement that Al partially (10%) substitutes for As in the tetrahedral sites (Grey *et al*., 2014*b*). The As deficit is much smaller (3%) in penberthycroftite and substitution of Al for As could not be verified in the structure refinement. By analogy with bariopharmacoalumite, we have assigned the excess Al to the As site, giving an empirical

https://doi.org/10.1180/minmag.2016.080.069 Published online by Cambridge University Press

TABLE 4. Refined coordinates, site occupancy factors (SOF), isotropic displacement parameters (Å^2) and calculated bond-valence sums (BVS) in penberthycroftite.

	SOF	*x*	*y*	*z*	U_{iso}	BVS
Heteropolyhedral layer atom sites						
As1	1	0.4882(2)	0.67773(5)	0.33708(8)	0.0330(3)	5.3
As2	1	0.9798(2)	0.58554(5)	0.36977(8)	0.0340(4)	5.2
As3	1	0.2789(2)	0.72174(5)	0.07415(8)	0.0341(4)	5.1
Al1	1	0.0930(5)	0.6835(1)	0.2379(2)	0.0334(9)	2.8
Al2	1	0.6413(5)	0.5841(1)	0.4701(2)	0.0301(8)	2.8
Al3	1	0.6127(5)	0.5559(1)	0.2800(2)	0.0334(9)	2.8
Al4	1	0.3499(5)	0.6068(1)	0.1680(2)	0.0333(9)	2.8
Al5	1	0.3998(5)	0.6606(1)	0.5369(2)	0.0323(9)	2.9
Al6	1	0.1185(5)	0.7102(1)	0.4213(2)	0.0354(9)	2.8
O1	1	0.3414(11)	0.6657(3)	0.2551(5)	0.034(2)	2.0
O2	1	0.5902(11)	0.6200(3)	0.3573(5)	0.036(2)	2.1
O3	1	0.3699(13)	0.6907(3)	0.4216(6)	0.044(2)	2.0
O4	1	0.6219(11)	0.7255(3)	0.3161(5)	0.033(2)	1.5
O5	1	0.8840(12)	0.5861(4)	0.4613(6)	0.045(2)	1.8
O6	1	0.8510(12)	0.5608(3)	0.2879(5)	0.041(2)	1.8
O7	1	1.0371(10)	0.6507(3)	0.3476(5)	0.028(2)	2.0
O8	1	1.1512(12)	0.5471(3)	0.3822(5)	0.041(2)	1.5
O9	1	0.3636(12)	0.6603(3)	0.0830(5)	0.039(2)	1.8
O10	1	0.1743(11)	0.7250(3)	–0.0235(5)	0.032(2)	1.8
O11	1	0.4306(12)	0.7694(3)	0.0836(5)	0.041(2)	1.8
O12	1	0.1286(12)	0.7318(3)	0.1466(5)	0.039(2)	1.7
OH1	1	0.1093(11)	0.6181(3)	0.1772(5)	0.030(2)	0.95
OH2	1	0.1122(12)	0.7416(3)	0.3144(5)	0.037(2)	1.05
OH3	1	0.6377(11)	0.6501(3)	0.5339(5)	0.034(2)	0.95
OH4	1	0.4106(11)	0.5892(3)	0.4923(5)	0.033(2)	1.0
OH5	1	0.6034(12)	0.5243(3)	0.3952(6)	0.044(2)	0.85
OH6	1	0.5894(11)	0.5973(3)	0.1842(5)	0.035(2)	1.1
OH7	1	0.3681(10)	0.5541(3)	0.2553(5)	0.029(2)	0.95
OH8	1	0.1617(11)	0.6668(3)	0.5181(5)	0.035(2)	1.05
Ow1	1	–0.1408(13)	0.6914(3)	0.2101(6)	0.043(2)	0.55
Ow2	1	0.6701(12)	0.5365(3)	0.5669(6)	0.045(2)	0.45
Ow3	1	0.6370(13)	0.4880(4)	0.2209(6)	0.052(3)	0.45
Ow4	1	0.3128(13)	0.5562(3)	0.0769(6)	0.053(2)	1.1
Ow5	1	0.3803(11)	0.6293(3)	0.6451(5)	0.035(2)	0.5
Ow6	1	–0.1195(13)	0.7225(4)	0.4367(6)	0.046(2)	0.45
S1	0.304(9)	0.3734(13)	0.5106(3)	0.0309(6)	0.053(2)	5.8
Os1	0.304(9)	0.251(2)	0.4983(7)	–0.0407(10)	0.053(2)	1.6
Os2	0.304(9)	0.391(3)	0.4642(5)	0.0873(11)	0.053(2)	1.6
Os3	0.304(9)	0.540(2)	0.5233(7)	–0.0004(13)	0.053(2)	1.6
Interlayer water molecules						
W1	1	0.7300(14)	0.7843(4)	0.5478(6)	0.056(1)	
W2	1	0.8916(14)	0.4450(4)	0.3886(6)	0.056(1)	
W3	1	0.4024(14)	0.6873(4)	0.7890(6)	0.056(1)	
W4	1	0.9351(14)	0.6766(4)	0.6447(6)	0.056(1)	
W5	0.70(2)	0.549(2)	0.6375(6)	–0.0580(9)	0.056(1)	
W6	0.35(2)	0.107(4)	0.4125(11)	0.9412(16)	0.056(1)	
W7	0.43(2)	0.075(3)	0.6218(10)	0.9277(15)	0.056(1)	
W8	0.28(2)	0.959(5)	0.4654(14)	0.177(2)	0.056(1)	
W9	0.28(2)	0.350(5)	0.4247(15)	0.226(2)	0.056(1)	
W10	0.32(2)	0.180(4)	0.3461(11)	0.1940(18)	0.056(1)	

https://doi.org/10.1180/minmag.2016.080.069 Published online by Cambridge University Press

TABLE 5. Polyhedral bond distances (Å) in penberthycroftite.

As1–O1	1.680(8)	As2–O5	1.663(9)	As3–O9	1.653(8)
As1–O2	1.649(8)	As2–O6	1.683(8)	As3–O10	1.682(8)
As1–O3	1.697(10)	As2–O7	1.710(7)	As3–O11	1.663(9)
As1–O4	1.620(8)	As2–O8	1.632(9)	As3–O12	1.704(9)
Av.	1.661	Av.	1.672	Av.	1.675
Al1–O1	1.974(9)	Al3–O2	2.007(9)	Al5–O3	1.953(9)
Al1–O7	1.978(8)	Al3–O6	1.847(10)	Al5–O11	1.885(9)
Al1–O12	1.899(9)	Al3–OH5	1.973(10)	Al5–OH3	1.867(9)
Al1–OH1	1.884(8)	Al3–OH6	1.815(9)	Al5–OH4	1.899(9)
Al1–OH2	1.868(9)	Al3–OH7	1.908(9)	Al5–OH8	1.855(9)
Al1–Ow1	1.844(10)	Al3–Ow3	1.930(10)	Al5–Ow5	1.880(9)
Av.	1.908	Av.	1.913	Av.	1.890
Al2–O2	1.992(9)	Al4–O1	1.999(9)	Al6–O3	2.007(10)
Al2–O5	1.897(10)	Al4–O9	1.884(9)	Al6–O7	1.945(8)
Al2–OH3	1.914(8)	Al4–OH1	1.902(9)	Al6–O10	1.855(9)
Al2–OH4	1.852(9)	Al4–OH6	1.871(10)	Al6–OH2	1.845(9)
Al2–OH5	1.896(9)	Al4–OH7	1.887(8)	Al6–OH8	1.867(9)
Al2–Ow2	1.920(9)	Al4–Ow4	1.903(9)	Al6–Ow6	1.903(11)
Av.	1.912	Av.	1.908	Av.	1.904
S1–O26	1.43(1)				
S1–Os1	1.45(2)				
S1–Os2	1.45(2)				
S1–Ow4	1.45(2)				
Av.	1.44				

formula: $[Al_{5.96}Fe_{0.04}(As_{0.97}Al_{0.03}O_4)_3(SO_4)_{0.26}(OH)_{8.30}(H_2O)_{5.44}](H_2O)_{7.8}$.

Although the H atoms were not located in the refinement of penberthycroftite, the different H-containing species are readily identified from the bond-valence sums reported in Table 4. On this basis OH1 to OH8 are assigned as hydroxyl ions and Ow1 to Ow6 are coordinated water molecules.

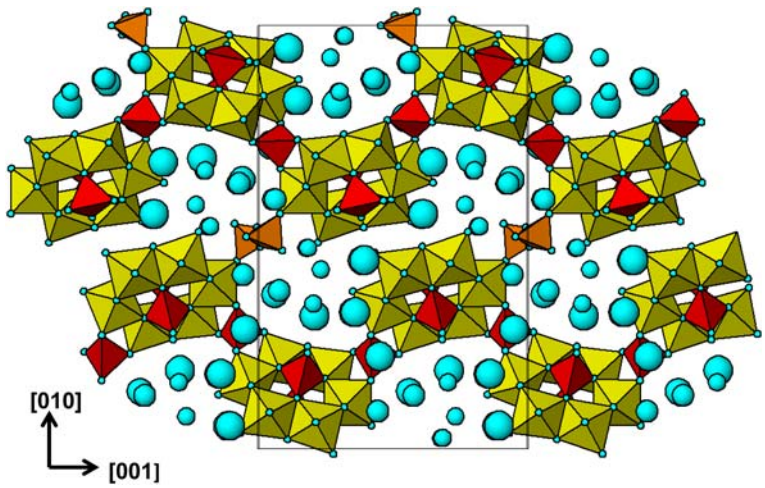

FIG. 5. Projection of the penberthycroftite structure along [100]. Interlayer water molecules are shown as blue spheres, with sizes proportional to the site occupancies. Sulfate tetrahedra are brown. Arsenate tetrahedra are red.

https://doi.org/10.1180/minmag.2016.080.069 Published online by Cambridge University Press

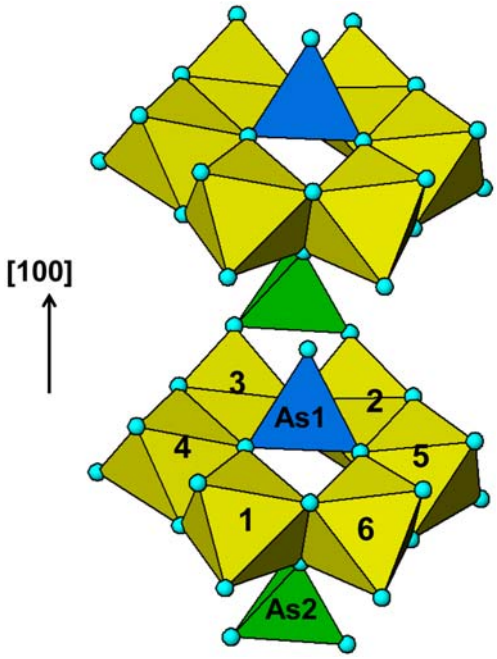

FIG. 6. Polyoxometallate clusters in penberthycroftite. The independent Al-centred octahedra are labelled 1 to 6.

The sites W1 to W10 are all interlayer water molecules. The site Ow4, a terminal anion of the octahedron around Al4, is more complicated because the SO_4 group, with 30% occupancy, is bonded to this anion. Thus this site is expected to be 0.3 O^{2-} + 0.7 H_2O. The formula from the refined site occupancies is $[Al_6(AsO_4)_3(SO_3)_{0.3}(OH, H_2O)_{14}](H_2O)_{6.4}$, which is quite close to the empirical formula except for the higher interlayer water content in the latter. The higher water content obtained from the thermogravimetric analysis probably includes interlayer sorbed water that is mobile and could not be located during the refinement from difference Fourier maps.

Pairs of O atoms most likely to be involved in H-bonding are listed in Table 6. Distances involving pairs of sites that are both partially occupied have not been included and an upper cut-off of 3 Å has been used. The As1- and As2-centred tetrahedra each have one non-bridging anion, O4 and O8, respectively, both of which are highly undersaturated, with a BVS of 1.5. Both of these anions have their valence requirements met by being acceptors for three H-bonds, from Ow1, Ow6, W3 and OH4, OH7 and Ow2, respectively. The O···O distances range from 2.58(1) to 2.75(1) Å, corresponding to strong bonds according to Libowitzky (1999). A strong H-bond also forms a bridge between adjacent heteropolyhedral layers, OH5···Ow2 = 2.70(1) Å. Interlayer water molecules form medium to strong H-bonds bonds with each other and with coordinated O, OH and Ow species. The diversity and strength of the H-bonding indicated in Table 6 is consistent with the very broad O–H stretching region in the infrared spectrum shown in Fig. 4. Using the correlation between O···O distances and O–H stretching frequencies established by Libowitzky (1999) the weak sharp peaks located below 3000 cm^{-1} correspond to the O···O distances in Table 6 that are ≤ 2.65 Å. These all involve a coordinated water or hydroxyl ion. The broad plateau between 3000 and 3400 cm^{-1} corresponds

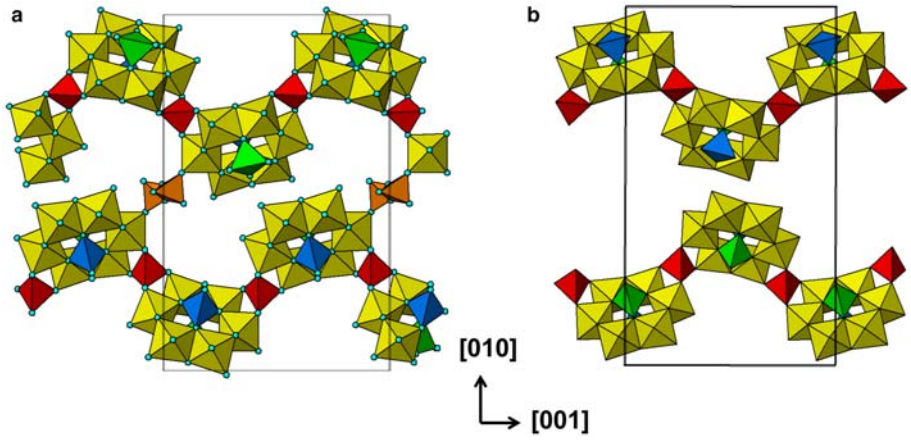

FIG. 7. Comparison of the heteropolyhedral layers in (*a*) penberthycroftite and (*b*) bettertonite, projected along [100].

https://doi.org/10.1180/minmag.2016.080.069 Published online by Cambridge University Press

TABLE 6. Hydrogen bonding in penberthycroftite.

OH1···W6	2.53(3)	W1···O11	2.77(1)
OH2···W3	2.90(1)	W1···W5	2.85(2)
OH3···W4	2.86(1)	W2···O5	2.92(1)
OH4···O8	2.75(1)	W3···O4	2.75(1)
OH5···Ow2	2.70(1)	W3···W5	2.87(2)
OH5···W2	2.98(1)	W4···O12	2.72(1)
OH7···O8	2.70(1)	W4···W10	2.81(3)
OH8···W4	2.75(1)	W5···O9	2.77(2)
Ow1···O4	2.70(1)	W7···O10	2.74(2)
Ow1···W1	2.72(1)		
Ow2···O8	2.58(1)		
Ow3···W8	2.71(4)		
Ow3···W9	2.64(4)		
Ow5···W2	2.82(1)		
Ow5···W3	2.67(1)		
Ow6···O4	2.65(1)		
Ow6···W1	2.65(1)		

to O···O distances between 2.65 and 2.80 Å. From Table 6 it is seen that most of the O···O distances in this range involve the interlayer water molecules.

Penberthycroftite is related closely, both compositionally and structurally, to bettertonite, $[Al_6(AsO_4)_3(OH)_9(H_2O)_5]\cdot 11H_2O$. Both minerals have the same layer composition and layer topology. The penberthycroftite structure can be derived from the bettertonite structure by a sliding of the layers relative to one another by ~6 Å along [001] coupled with a shrinking of the interlayer separation along [010] from 13.5 Å (=0.5*b*) to 12.3 Å. The resulting decrease in interlayer volume is accompanied by a decrease in the interlayer water content from 11 to 8 H_2O pfu. Both minerals can be described as polyoxometallates where the polyoxometallate cluster is a hexagonal ring of edge-shared octahedra with an AsO_4 tetrahedron attached to one side of the ring by corner-sharing, shown in Fig. 6. This type of cluster has recently been reported as a new polyoxometalate building block for the cluster composition $[VMo_6O_{25}]^{9-}$ (Gao *et al*., 2014). These polyoxometalate clusters, of composition $[AsAl_6O_{11}(OH)_9(H_2O)_5]^{8-}$, are interconnected along [100] and [001] by corner-sharing with other AsO_4 tetrahedra. The structures of the two minerals are compared in Fig. 7 and their properties are compared in Table 7. They are most readily distinguished by their different powder XRD patterns. The positioning of the crankshaft-like {010} layers in the two minerals results in the electron density being concentrated in {021} layers in penberthycroftite but in {011} layers in bettertonite and so *d*(021) at 9.73 Å is the strongest peak in the penberthycroftite XRD pattern whereas *d*(011) at 13.65 Å is the strongest peak in the pattern for bettertonite.

Acknowledgements

We thank Cameron Davidson and Matthew Glenn for sample preparation and scanning electron microscopy assistance. We thank Robert Neller for the optical

TABLE 7. Comparative data for penberthycroftite and bettertonite.

	Penberthycroftite	Bettertonite
Formula (simplified)	$[Al_6(AsO_4)_3(OH)_9(H_2O)_5]\cdot 8H_2O$	$[Al_6(AsO_4)_3(OH)_9(H_2O)_5]\cdot 11H_2O$
Symmetry	Monoclinic, $P2_1/c$	Monoclinic $P2_1/c$
Cell (from single crystal, 100 K)	$a = 7.753(2)$, $b = 24.679(5)$, $c = 15.679(3)$ Å, $\beta = 94.19(3)°$ $Z = 4$, $V = 2991.9(1.2)$ Å^3	$a = 7.773(2)$, $b = 26.991(5)$, $c = 15.867(3)$ Å, $\beta = 94.22(3)°$ $Z = 4$, $V = 3319.9(1.2)$ Å^3
d_{calc}	2.18 g/cm^3	2.03 g/cm^3
Strongest powder pattern lines *d, I, hkl*	13.264, 46, (011) 12.402, 16, (020) 9.732, 100, (021) 7.420, 28, (110) 5.670, 8, (130) 5.423, 6, (1̄31)	13.648, 100 (011) 13.505, 50, (020) 7.805, 50, (031) 7.461, 30, (110) 5.880, 20, (130) 3.589, 20, (2̄02)
Optics	Minimum and maximum refractive indices 1.520(1) and 1.532(1)	Biaxial (+) $\alpha = 1.515(1)$, $\beta = 1.517(1)$, $\gamma = 1.523(1)$
Fluorescence	Non fluorescent in short and long wavelength UV	Non fluorescent in short and long wavelength UV

https://doi.org/10.1180/minmag.2016.080.069 Published online by Cambridge University Press

image in Fig. 1. The single crystal data was collected at the macromolecular MX2 beamline at the Australian Synchrotron, Clayton, Victoria. Thanks to Dr. Helen Brand at the powder diffraction beamline of the Australian Synchrotron for collecting the powder XRD data.

References

Betterton, J. (2000) Famous mineral localities: Penberthy Croft mine, St. Hilary, Cornwall, England. *UK Journal of Mines and Minerals*, **20**, 7–37.

Bevins, R.E., Young, B., Mason, J.S., Manning, D.A.C. and Symes, R.F. (2010). *Mineralization of England and Wales.* Geological Conservation Review Series, No 36. Joint Nature Conservation Committee, Peterborough, UK, pp. 496–499.

Bowell, R.J., Alpers, C.N., Jamieson, H.E., Nordstrom, D.K. and Majzlan, J. (editors) (2014) *Arsenic: Environmental Geochemistry, Mineralogy, and Microbiology.* Reviews in Mineralogy and Geochemistry, 79. Mineralogical Society of America and the Geochemical Society, Chantilly, Virginia, USA, 635 pp.

Cooper, M.A., Abdu, Y.A., Ball, N.A., Hawthorne, F.C., Back, M.E., Tait, K.T., Schlüter, J., Malcherek, T., Pohl, D. and Gebhard, G. (2012). Ianbruceite, ideally $[Zn_2(OH)(H_2O)(AsO_4)](H_2O)_2$, a new arsenate mineral from the Tsumeb mine, Otjikoto (Oshikoto) region, Namibia: description and crystal structure. *Mineralogical Magazine*, **76**, 1119–1131.

Farrugia, L.J. (2012) WinGX and ORTEP for Windows: an update. *Journal of Applied Crystallography*, **45**, 849–854.

Frost, R.L., Scholz, R. and Lopez, A. (2015) Raman and spectroscopic characterization of the arsenate-bearing mineral tangdanite and in comparison with the discredited mineral clinotyrolite. *Journal of Raman Spectroscopy*, **46**, 920–926.

Gao, Q., Li, F., Wang, Y., Xu, L., Bai, J. and Wang, Y. (2014) Organic functionalization of polyoxometalate in aqueous solution: self-assembly of a new building block of $\{VMo_6O_{25}\}$ with triethanolamine. *Dalton Transactions*, **43**, 941–944.

Grey, I.E., Mumme, W.G., MacRae, C.M., Caradoc-Davies, T., Price, J.R., Rumsey, M.S. and Mills, S.J. (2013) Chiral edge-shared octahedral chains in liskeardite, $[(Al,Fe)_{32}(AsO_4)_{18}(OH)_{42}(H_2O)_{22}]\cdot 52H_2O$, an open framework mineral with a pharmacoalumite-related structure. *Mineralogical Magazine*, **77**, 3125–3135.

Grey, I.E., Kampf, A.R., Price, J.R. and MacRae, C.M. (2014*a*) Bettertonite, IMA 2014-074. CNMNC Newsletter No. 23, February 2015, page 55; *Mineralogical Magazine*, **79**, 51–58.

Grey, I.E., Mumme, W.G., Price, J.R., Mills, S.J., MacRae, C.M. and Favreau, G. (2014*b*) Ba–Cu ordering in bariopharmacoalumite-*Q2a2b2c* from Cap Garonne, France. *Mineralogical Magazine*, **78**, 851–860.

Grey, I.E., Betterton, J., Kampf, A.R., Price, J.R. and MacRae, C.M. (2015*a*) Penberthycroftite, IMA 2015-025. CNMNC Newsletter No. 26, August 2015, page 943; *Mineralogical Magazine*, **79**, 941–947.

Grey, I.E., Kampf, A.R., Price, J.R. and MacRae, C.M. (2015*b*) Bettertonite, $[Al_6(AsO_4)_3(OH)_9(H_2O)_5]\cdot 11H_2O$, a new mineral from the Penberthy Croft mine, St. Hilary, Cornwall, UK, with a structure based on polyoxometalate clusters. *Mineralogical Magazine*, **79**, 1849–1858.

Laugier, J. and Bochu, B. (2000) *LMGP-Program for the Interpretation of X-ray Experiments.* INPG/ Laboratoire des Matériaux et du Génie Physique. St Martin d'Heres, France.

Libowitzky, E. (1999) Correlation of O–H stretching frequencies and O–H···O hydrogen bond lengths in minerals. Pp. 103–115 in: *Hydrogen Bond Research* (P. Schuster and W. Mikenda, editors). Springer-Verlag Wien.

Majzlan, J., Alpers, C.N., Koch, C.B., McCleskey, R.B., Myneni, S.C.B. and Neil, J.M. (2011) Vibrational, X-ray absorption, and Mossbauer spectra of sulphate minerals from the weathered massive sulphide deposit at iron Mountain, California. *Chemical Geology*, **284**, 296–305.

Mandarino, J.A. (1981) The Gladstone-Dale relationship: Part IV. The compatibility concept and its application. *The Canadian Mineralogist*, **19**, 441–450.

Nakamoto, K. (1970) *Infrared Spectra of Inorganic and Coordination Compounds.* Wiley-Interscience, New York, 338 pp.

Petříček, V. and Dušek, M. (2006) *JANA2006. Structure Determinations Software Programs.* Institute of Physics, Academy of Sciences of the Czech Republic, Prague.

Sheldrick, G.M. (2008) A short history of SHELX. *Acta Crystallographica*, **A64**, 112–122.

Taylor, R. (2011) *Gossans and Leached Cappings Field Assessment.* Springer Verlag, Heidelberg, Germany, 146 pp.

Vansant, F.K., van der Veken, B.J. and Dessyn, H.O. (1973) Vibrational analysis of arsenic acid and its anions. 1. Description of the Raman spectra. *Journal of Molecular Structure*, **15**, 425–437.

Visser, J.W. (1969) A fully automated program for finding the unit cell from powder data. *Journal of Applied Crystallography*, **2**, 89.

Walenta, K. (1983) Bulachit, ein neues Aluminiumarsenatmineral von Neubulach im nordlichen Schwarzwald. *Aufschluss*, **34**, 445–451.